Study on the Interactions of Kaempferol and Quercetin with Intravenous Immunoglobulin by Fluorescence Quenching, Fourier Transformation Infrared Spectroscopy and Circular Dichroism Spectroscopy

Yong-chun LIU,[a,b] Zheng-yin YANG,*[,a] Juan DU,[a] Xiao-jun YAO,[a] Rui-xia LEI,[b] Xu-dong ZHENG,[b] Jian-ning LIU,[b] Huai-sheng HU,[b] and Hong LI[b]

[a] *College of Chemistry and Chemical Engineering, State Key Laboratory of Applied Organic Chemistry, Lanzhou University; Lanzhou 730000, P. R. China: and* [b] *College of Chemistry and Chemical Engineering, Longdong University; Qingyang Gansu 745000, P. R. China.*

Received September 18, 2007; accepted January 16, 2008; published online January 22, 2008

The interactions of kaempferol and quercetin with intravenous immunoglobulin (IVIG) were studied *in vitro* by spectroscopic methods including fluorescence spectra, Fourier transformation infrared (FT-IR) spectra and circular dichroism (CD) spectra. The binding parameters for the reactions calculated according to the Sips equation suggested that the bindings of IVIG to kaempferol and quercetin were characterized by two binding sites with the average affinity constants K_0 at $1.032\times10^4\,\mathrm{M}^{-1}$ and $1.849\times10^4\,\mathrm{M}^{-1}$, respectively. The binding of IVIG with quercetin is stronger than that of IVIG with kaempferol. They were of non-specific and weak drug–protein interactions. Docking was used to calculate the interaction modes between kaempferol and quercetin with IVIG. The secondary structural compositions of free IVIG and its kaempferol, quercetin complexes were calculated by the FT-IR difference spectra, self-deconvolution, second derivative resolution enhancement and the curve-fitting procedures of amide I band respectively, which are in good agreement with the analyses of CD spectra. The effect of 3′-OH substituent in quercetin is distinct between the interactions of IVIG with kaempferol and quercetin for the secondary structure of the protein. The observed spectral changes indicate a partial unfolding of the protein structure, but the typical β structural conformation of IVIG is still retentive in the presence of both drugs in aqueous solution. The average binding distances between the chromophores of IVIG with kaempferol (4.30 nm) and quercetin (4.35 nm) were obtained on the basis of the theory of Förster energy transfer. IVIG can serve as transport protein (carrier) for kaempferol and quercetin.

Key words intravenous immunoglobulin; immune gamma globulin; kaempferol; quercetin; protein; interaction

Initially used as replacement therapy for patients with primary and secondary immune deficiencies, intravenous immunoglobulin (IVIG), the human serum immunoglobulin (Ig) fraction that is mainly composed of normal human polyclonal IgG obtained from plasma pools from a large number of healthy blood donors, is now widely used for the treatment of a large number of autoimmune and systemic inflammatory diseases.[1,2] Recently, great attention has been paid to IVIG potential use as adjuvant anti-neoplastic agent.[3—5] Studies on the anticancer alkaloid vindesine (VDS) conjugates of the anti-CEA (carcinoembryonic antigen) antibodies against a colorectal tumor xenograft revealed that antibody 14.95.55 (IgG2a) suppressed tumor growth both alone and as a VDS conjugate, while 11.285.14 (IgG1) produced only a slight effect alone but an almost complete and lasting suppression of tumor growth as a VDS conjugate. Acute studies showed that VDS-11.285.14 conjugate was considerably less toxic than free VDS in Balb/c mice.[6] It has been revealed that there are different transfer mechanism between the drug–protein conjugates and free drugs transferred into cells, and the conjugates can reduce the toxicity of drugs, resulting in a prolongation of survival time.[7] Studies on the efficacy of an IgG $F(ab)_2$ preparation against taxol-induced C activation revealed that at a therapeutically relevant dose level (10 mg/ml), this Fc-depleted IgG caused significant suppression of taxol-induced SC5b-9 formation, but replacing IVIG with 10 mg/ml human serum albumin (HSA) caused no inhibition of taxol-induced rise of SC5b-9.[8] Also, it is reported that within a range of molar concentration ratio of taxol to IVIG, the interaction of IVIG with taxol can inhibit taxol from crystallizing in aqueous solution.[9] Studies *in vitro* have revealed that IVIG may stimulate the production of IL-12, an anti-tumor and anti-angiogenic cytokine, and enhanced NK cell activity.[4] Studies also revealed that IVIG can decrease the level of matrix metalloproteinase-9 (MMP-9) expression in the U937 monocyte line with a decrease in the m-RNA level of MMP-9 that participates in basement membrane degradation, a vital step in the invasion of metastatic cancer cells. So, IVIG may serve as an adjuvant therapy in cancer due to its anti-neoplastic properties that may synergize with more specific MMP inhibitors and other anti-cancer drugs.[10,11] In addition, IgG presents itself in the blood of adults at 9.5—12.5 mg/ml, and as one of human plasma proteins, it is capable of binding an extraordinarily diverse range of metabolites, drugs, organic compounds and relevant antigens.[12—14] With the remarkable binding properties, IVIG can serve as an important transport protein for drugs, which may have important roles in the discovery of novel drug delivery system and targeted drug therapy. By using its high-safety profile, clinicians may construct new protocols for patients.

Flavonols are plant pigments that are ubiquitous in nature. Kaempferol (3,4′,5,7-pentahydroxyflavone), quercetin (3,3′,4′,5,7-pentahydroxyflavone, Fig. 1) and other related plant flavonols have come into recent prominence because of their usefulness as anticancer, antitumor, anti-AIDS, and other important therapeutic activities of significant potency and low systemic toxicity.[15—18] It is non-specific and reversible that many of these agents bind to serum proteins, and the binding affects their pharmacological and pharmacokinetic properties.[12] Therefore a study on the binding of

* To whom correspondence should be addressed. e-mail: yangzy@lzu.edu.cn

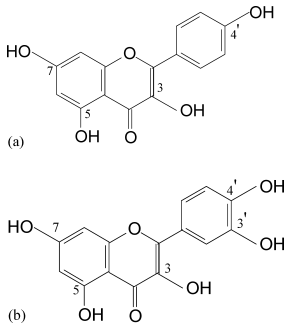

Fig. 1. The Chemical Structures of Kaempferol (a) and Quercetin (b)

IVIG to flavonols is very significant. In addition, the only difference of chemical structure between kaempferol and quercetin is that there is a 3′-OH substituent in quercetin but there is not in kaempferol, which may cause some significant substituent effects for their interactions with proteins. Previously, the binding of kaempferol and quercetin to HSA were studied, but serum albumin and IgG are different proteins with different binding features to various drugs.[16,17] Furthermore, the interaction of IVIG with drugs in fact represents the behavior of IgG and it is of much more clinical use.

Experimental

Materials Intravenous immunoglobulin (IVIG, medical name: lyophilized human immunoglobulin (pH 4) for intravenous injection, component of IgG ≥95%, M_r 150 kDa) was obtained from Lanzhou Pharmaceutical Co., Ltd., China. Kaempferol and quercetin (standard sample, purity ≥98%) were obtained from Chengdu Scholar Bio-Tech. Co., Ltd., China. 1.0 M NaCl solution was used to keep the ion strength at 0.1. Tris–HCl buffer was selected to keep the pH of the solution at 7.40. IVIG solution of 1.0×10^{-4} M was prepared in pH 7.40 Tris–HCl buffer solution and stored at 275—281 K until it was used. Kaempferol and quercetin solution (1.0 mM) were prepared by dissolving them in ethanol, respectively. All other chemicals were of analytical reagent grade.

Methods Fluorescence spectra were recorded using RF-4500 spectrofluorophotometer (Hitachi) with a 1 cm quartz cell. Both the excitation and emission band widths were 5 nm. The intrinsic fluorescence of IVIG was obtained at 337 nm when exited at 283 nm. A quantitative analysis of potential interaction between drug and IVIG was performed by fluorimetric titration, that is, 3 ml solution containing 1.0 μM IVIG was titrated by successive additions of drug solution at 5 μl every time to give a final concentration of 32.26 μM. All experiments were measured after 5 min at a constant room temperature, 296 K.

The binding parameters were calculated using the Sips procedure, which is based on the following equation[19]:

$$r = \frac{n(K_o c)^{\alpha}}{1 + (K_o c)^{\alpha}} \quad (1)$$

$$\lg \frac{r}{n - r} = \alpha \lg c + \alpha \lg K_o \quad (2)$$

Where r is the moles of drug bound per mole of protein; K_o is the average affinity constant accurately equal to the median affinity; c is the molar concentration of free drug; α is the index of affinity heterogeneity of IVIG. n is the number of binding sites. The dependence of $\lg\{r/(n-r)\}$ on the logarithmic value of the free quencher concentration c is linear with slope equal to the value of α, and then K_o can be calculated from the intercept.

Quenching data were also analyzed according to the Stern–Volmer equation, which could be used to determine the fluorescent quenching mechanism[20,21]:

$$F_o/F = 1 + K_q \tau_o [Q] = 1 + K_{SV}[Q] \quad (3)$$

Where F_o and F are the fluorescence intensity in the absence and in the presence of drug at [Q] concentration respectively; K_{SV} is the Stern–Volmer dynamic quenching constant; K_q is the quenching rate constant of bimolecular diffusion collision; τ_o is the average fluorescence lifetime of biological macromolecules; [Q] is the molar concentration of drug.

FT-IR measurements were carried out at a constant room temperature (296 K) on a Nicolet Nexus 670 FT-IR spectrometer (America) equipped with a germanium attenuated total reflection (ATR) accessory, a DTGS KBr detector and a KBr beam splitter. All spectra were taken *via* the ATR method with resolution of 4 cm^{-1} and 60 scans. Spectra processing procedures: spectra of buffer solution were collected at the same condition, then, subtract the absorbance of buffer solution from the spectra of sample solution to get the FT-IR difference spectra of proteins. The subtraction criterion was that the original spectra of protein solution between 2200 cm^{-1} and 1800 cm^{-1} was featureless,[22] that is, no characteristic peaks between 2200 cm^{-1} and 1800 cm^{-1} appear and the curve is flatness. The secondary structural compositions of free IVIG and its drug complexes were calculated by the FT-IR difference spectra, self-deconvolution, second derivative resolution enhancement and the curve-fitting procedures of amide I band. The resulting curve fitted is analyzed as following: Each Lorentzian band is assigned to a secondary structure according to the frequency of its maximum; β-antiparallel: 1684—1696 cm^{-1}; turn: 1662—1679 cm^{-1}; β-sheet: 1620—1637 cm^{-1}; α-helix: 1649—1659 cm^{-1}; random coil: 1640—1646 cm^{-1}. The area of all the component bands assigned to a given conformation is then summed and divided by the total area. The number obtained is taken as the proportion of the polypeptide chain in that conformation.[23]

Far-ultraviolet CD spectra were measured at a constant temperature (296 K) on an Olis RSM 1000 CD spectrophotometer (U.S.), and the optical path length was 0.2 cm. The induced ellipticity was defined as the ellipticity of the drug–IVIG mixture minus the ellipticity of drug alone at the same wavelength. CD results were expressed in terms of mean residue ellipticity (MRE) in mdeg cm^2 $dmol^{-1}$ according to the following equation[24]:

$$[\theta]^{MRE} = \frac{\text{observed CD (mdeg)}}{Cp \times n \times l \times 10} \quad (4)$$

Where Cp is the molar concentration of the protein, n is the number of amino acid residues (670) and l is the path length (0.2 cm).

Ultraviolet–visible spectra were recorded on a Lambda 35 UV/VIS spectrometer (Perkin Elmer).

Docking study of the binding mode between drug and human IgG was performed on SGI Fuel workstation. The 3D structure of human IgG in complex with 5-(*para*-nitrophenyl phosphonate)-pentanoic acid was downloaded from the Brookhaven Protein Data Bank (PDB entry code 1AJ7). The initial structure of drug was generated by molecular modeling software Sybyl 6.9.1.[25] The geometry was subsequently optimized using the Tripos force field with Gasteiger–Huckel charges. The FlexX program was used to calculate the interaction mode between drug and human IgG. During docking process, a maximum of 30 conformers was considered for the compound. The conformer with the lowest binding free energy was used for further analysis.

Results and Discussion

Analysis of Fluorescence Quenching of IVIG by Drugs When exited at 283 nm, IVIG shows a characteristic emission maximum at 337 nm mainly due to its tryptophan (Trp) residues. Both of the addition of a solution of drugs to IVIG solution caused decreases in the emission at 337 nm upon excitation at 283 nm as shown in Fig. 2, and the fluorescence emission maximum wavelength of IVIG shifted to a shorter wavelength. The wavelength strongly depends on the microenvironment especially the hydrophobicity around the protein, so the fluorescence emission wavelength was also estimated for the binding mode. Both the maximum emission wavelengths of IVIG shift toward shorter wavelengths when the solutions of two drugs were added respectively, indicating that the two drugs were accessible and bound to the chromophores of hydrophobic cleft of the protein, which were placed in a more hydrophobic environment as the molecules of water were pushed out from the hydrophobic binding domain after the addition of both drugs, respectively.[26]

In the experiment of fluorimetric titration of kaempferol into IVIG solution, the Stern–Volmer dynamic quenching

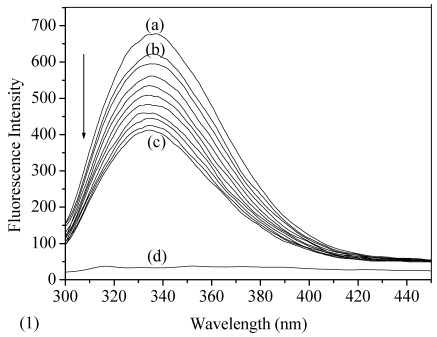

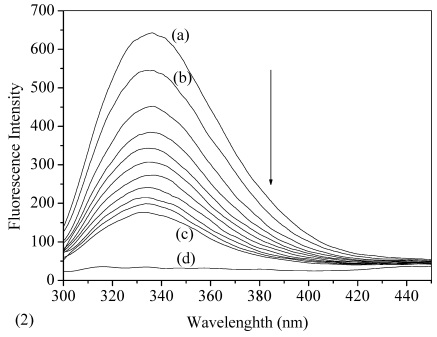

Fig. 2. Fluorescence Spectra of IVIG–Kaempferol (1) and IVIG–Quercetin (2) Systems at 296 K, pH 7.40

The molar concentration of IVIG was 1.0 μM and both the molar concentrations of drugs increased from 0 to 16.39 μM from (a) to (c). (d) Molar concentrations of both free drugs were 32.26 μM. λ_{ex}=283 nm, λ_{em}=337 nm.

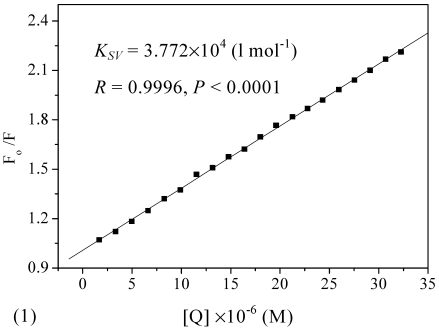

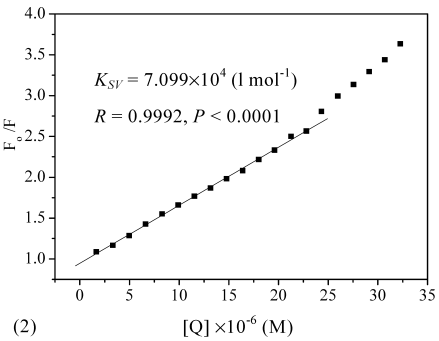

Fig. 3. Stern–Volmer Plots for the Kaempferol–IVIG (1) and Quercetin–IVIG (2) Systems at 296 K, pH 7.40

IVIG concentration was 1.0 μM; λ_{ex}=283 nm, λ_{em}=337 nm.

constant, $K_{SV}=3.772\times10^4$ (l mol^{-1}), was calculated from the good linear relationship between F_o/F and the concentration of quencher which increased from 1.664 to 32.26×10^{-6} M as shown in Fig. 3 (1), then $K_q=3.772\times10^{12}$ (l mol^{-1} s^{-1}) was calculated when τ_o was taken as 10^{-8} (s^{-1}).[20,21] Similarly to the method of kaempferol, in the experiment of fluorimetric titration of quercetin into IVIG solution, its Stern–Volmer dynamic quenching constant, $K_{SV}=7.099\times10^4$ (l mol^{-1}), was calculated from the good linear relationship between F_o/F and the concentration of quencher which increased from 1.664 to 22.80×10^{-6} M as shown in Fig. 3 (2), then $K_q=7.099\times10^{12}$ (l mol^{-1} s^{-1}) was calculated when τ_o was taken as 10^{-8} (s^{-1}). Both of the current values of K_q are much greater than that of $K_{q(max)}$ (2.0×10^{10} l mol^{-1} s^{-1}), the maximum quenching rate constant of bimolecular diffusion collision, indicating that there were indicative of a static type of quenching mechanism arisen from the formation of dark complex between the fluorophore and quenching agents, and the quenching constant can be interpreted as the association or binding constant of the complexation reaction.[20,21] From the values of both quenching constant, it will be predicted that the interaction of IVIG with quercetin is stronger than that of IVIG with kaempferol. However, the Stern–Volmer plots for quercetin–IVIG system were inclined gradually to the F_o/F axis as shown in Fig. 3 (2) when the concentration of quercetin increased, especially in higher concentrations, which indicates that the main static type of quenching mechanism accompanied by a minor dynamic one. This may be caused by the effect of 3′-OH substituent of quercetin in comparison with kaempferol.

The binding parameters for the drug–IVIG interactions were estimated by Sips plots (Fig. 4) and summarized in Table 1, which shows good linear correlations when the number of binding sites was taken as 2 and 4. The most binding sites of IgG for antigen are located in complement-determining region (CDR) of antigen-binding fragments (Fab), and the crystallizable fragments (Fc) can be considered to a certain extent as a similarity to Fab region and can also bind to smaller molecules.[13,14] Additionally, the framework region (FR), which consists of FR1, FR2, FR3 and FR4, provides a supporting framework for CDR of Fab of IgG. Recently studies have revealed that FR3 adjacent to binding site for antigen can also bind to antigens directly.[28,29] It is inferred that IgG probably has more potential binding sites for antigens/semi-antigens.[30] Figure 4 and Table 1 show that the Sips plots display better linear correlations whether the number of binding sites (n) is 2 or 4, and both of the affinity constants present at the order of magnitude about 10^4 M^{-1}, indicating that they are of non-specific and weak interactions with respect to the other strong ligand–protein complexes with the binding constants ranging from 10^6 to 10^8 M^{-1},[31] and that the binding sites of IVIG for the two drugs are probably the two antigen-binding fragments (Fab) and the two crystallizable fragments (complement-binding sites, Fc).[27] The non-specific and weak interactions between the protein with drugs indicate that IVIG can be used as transport protein (carrier) for kaempferol and quercetin in comparison with the mode of covalent interaction. It is known that the two semi-antigen binding sites located respectively in two CDRs of Fab regions of IgG appear stronger affinity than other binding regions including the two Fc regions. When n=2, the affinity constant K_o was the average value of two Fab regions binding to drugs; when n=4, the affinity constant K_o was the average

Table 1. Binding Parameters of IVIG with Kaempferol and Quercetin Measured by Fluorimetric Titration at 296 K, pH 7.40

	Kaempferol				Quercetin			
	$K_o\times10^4$ (M^{-1})	a	R	p	$K_o\times10^4$ (M^{-1})	a	R	p
$n=2$	1.032	0.8239	0.9976	<0.0001	1.849	0.8598	0.9944	<0.0001
$n=4$	0.3170	0.7653	0.9961	<0.0001	0.5035	0.7753	0.9909	<0.0001

n is the number of the binding sites.

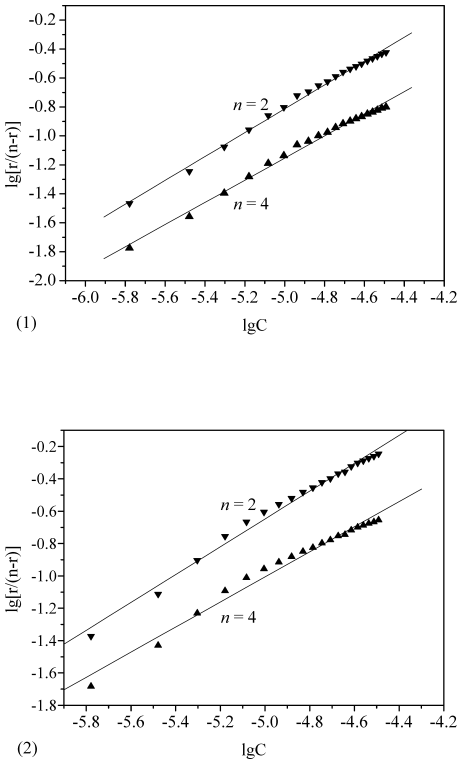

Fig. 4. The Sips Plots for the Kaempferol–IVIG (1) and Quercetin–IVIG (2) Systems at 296 K, pH 7.40

IVIG concentration was 1.0 μM. λ_{ex}=283 nm, λ_{em}=337 nm. The number of binding sites was taken as 2 (▼) and 4 (▲).

one of two Fab regions and two Fc regions binding to drugs simultaneously. So the K_o value decreased drastically as n increased from 2 to 4. However, the average affinity constant (K_o) was higher when n=2 than when n=4 for both drugs, indicating that Fab regions of IgG appear stronger affinities than Fc regions. Hence, the main binding sites of IVIG to the two drugs are the two CDRs of Fab regions. Furthermore, the average affinity constant (K_o) of IVIG binding to quercetin is higher than that of IVIG binding to kaempferol whether the binding site number is 2 or 4, indicating that IVIG binding to quercetin is stronger than IVIG to kaempferol in the present experiment environments, and that the 3′-OH substituent of quercetin in comparison with kaempferol may play a key role in the interactions. On the other hand, human IgG presents affinity heterogeneity,[19] which is mainly attributed to the different affinities either between the subclasses (IgG1, IgG2, IgG3 and IgG4) or/and between the Fab binding sites and the Fc binding sites of the same subclass of IgG binding to drugs. As shown in Table 1, the values of the affinity heterogeneity index (α) are higher when n=2 than when n=4, indicating that the difference of affinity heterogeneity between the two CDRs of Fab regions is slighter than the two Fc regions when they bind to molecules of kaempferol and quercetin, and there are relative effects between these binding domains.

FT-IR Spectra In the IR region, the frequencies of bands due to the amide I, II and III vibrations are sensitive to the secondary structure of proteins. The amide I peak position occurs in the region of 1600—1700 cm^{-1} (mainly C=O stretch), amide II band in the region of 1600—1500 cm^{-1} (C–N stretch coupled with N–H bending mode) and amide III band in the region of 1300 cm^{-1} (N–H binding mode coupled with C–N stretch). Amide I band is useful and more sensitive to the change of protein secondary structure than amide II and amide III bands.[32,33] Here, only the FT-IR spectra of amide I band were carried out to investigate the changes of secondary structure of the protein in the presence and in the absence of both drugs. Figure 5 shows the FT-IR spectra of free IVIG and its drug complexes in Tris–HCl buffer solution at 296 K, including the difference spectra, self-deconvolution, second derivative resolution enhancement and the curve-fitting procedures of amide I band. As shown in Fig. 5a, free IVIG shows eight peak positions of amide I band at 1611.95 cm^{-1}, 1626.58 cm^{-1}, 1637.35 cm^{-1}, 1646.76 cm^{-1}, 1652.91 cm^{-1}, 1661.60 cm^{-1}, 1671.28 cm^{-1} and 1679.09 cm^{-1} according to its self-deconvolution. Figure 5b shows the free IVIG curve-fitting procedures of amide I band.

After addition of kaempferol, according to the self-deconvolution of IVIG–kaempferol complexes, the typical peak positions of amide I at 1687.27 cm^{-1}, 1666.91 cm^{-1}, 1640.38 cm^{-1} and 1608.33 cm^{-1} are observed when the molar concentration ratio of IVIG to kaempferol is 1 : 4 as showed in Fig. 5c. Figure 5d shows the curve-fitting procedures of amide I band of IVIG–kaempferol complexes when the molar concentration ratio of IVIG to kaempferol is 1 : 4. After addition of quercetin, according to the self-deconvolution of IVIG–quercetin complexes, the typical peak positions of amide I at 1657.93 cm^{-1} and 1633.72 cm^{-1} are observed when the molar concentration ratio of IVIG to quercetin is 1 : 4 as showed in Fig. 5e. Figure 5f shows the curve-fitting procedures of amide I band of IVIG–quercetin complexes when the molar concentration ratio of IVIG to quercetin is 1 : 4. The contents of secondary structural compositions of free IVIG and its drug complexes were calculated according to the curve-fitting procedures of amide I respectively[23] and summarized in Table 2. It is observed from Table 2 that when kaempferol was added into the IVIG solution and the molar concentration ratio of IVIG to kaempferol was 1 : 4, the contents of secondary structural compositions of IVIG changed apparently: β-antiparallel (1684—1696 cm^{-1}) increased from 5.90±1.14% to 13.37±0.46%; turn (1662—1679 cm^{-1})

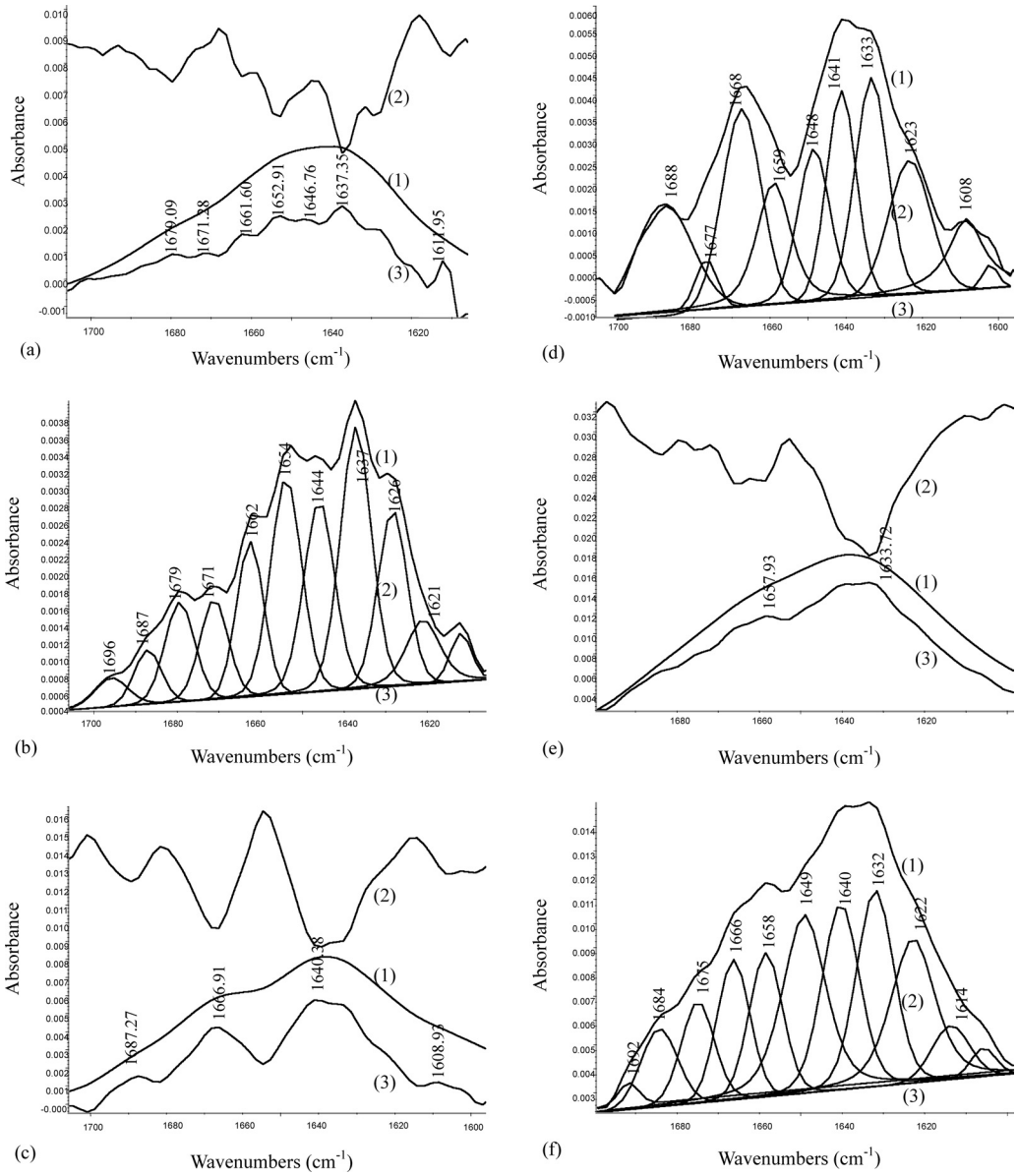

Fig. 5. The FT-IR Spectra of Free IVIG and Its Kaempferol and Quercetin Complexes at 296 K, pH 7.40

(a) Free IVIG difference spectroscopy (1), second derivative resolution enhancement (2) and self-deconvolution (3) of amide I band. IVIG concentration was 1.0 μM. (b) Free IVIG curve-fitting procedures of amide I band. (1) self-deconvolution; (2) curve-fitting results; (3) baseline of self-deconvolution spectra. IVIG concentration was 1.0 μM. (c) IVIG–kaempferol complex FT-IR spectra of amide I band. (1) difference spectroscopy; (2) second derivative resolution enhancement; (3) self-deconvolution. IVIG concentration was 1.0 μM and kaempferol concentration was 4.0 μM. (d) IVIG–kaempferol complex curve-fitting procedures of amide I band. (1) self-deconvolution; (2) curve-fitting results; (3) baseline of self-deconvolution spectra. IVIG concentration was 1.0 μM and kaempferol concentration was 4.0 μM. (e) IVIG–quercetin complex FT-IR spectra of amide I band. (1) difference spectroscopy; (2) second derivative resolution enhancement; (3) self-deconvolution. IVIG concentration was 1.0 μM and quercetin concentration was 4.0 μM. (f) IVIG–quercetin complex curve-fitting procedures of amide I band. (1) self-deconvolution; (2) curve-fitting results; (3) baseline of self-deconvolution spectra. IVIG concentration was 1.0 μM and quercetin concentration was 4.0 μM.

Table 2. Secondary Structural Compositions of IVIG and Its Kaempferol, Quercetin Complexes Estimated by the FT-IR Difference Spectra, Self-Deconvolution, Second Derivative Resolution Enhancement and the Curve-Fitting Procedures of Amide I Band at 296 K, pH 7.40

Amide I components	IVIG (1.0 μM)	IVIG (1.0 μM)+kaempferol (4.0 μM)	IVIG (1.0 μM)+quercetin (4.0 μM)
	(%)	(%)	(%)
β-Anti	5.90±1.14	13.37±0.46	6.95±0.14
Turn	24.29±0.30	20.51±0.70	16.96±0.34
β-Sheet	38.55±0.47	29.42±1.00	31.51±1.40
Remainders	31.27±0.39	36.70±1.25	44.57±0.96

decreased from 24.29±0.30% to 20.51±0.70%; β-sheet (1620—1638 cm^{-1}) decreased from 38.55±0.47% to 29.42±1.00%, while the remainders including α-helix (1654—1659 cm^{-1}) and random coil (1640—1648 cm^{-1}) increased from 31.27±0.39% to 36.70±1.25%. It is also observed from Table 2 that when quercetin was added into the IVIG solution and the molar concentration ratio of IVIG to quercetin was 1 : 4, the contents of secondary structural compositions of IVIG also changed apparently: β-antiparallel increased from 5.90±1.14% to 6.95±0.14%; turn decreased from 24.29±0.30% to 16.96±0.34%; β-sheet decreased from 38.55±0.47% to 31.51±1.40%, while the remainders including α-helix and random coil increased from 31.27±0.39% to 44.57±0.96%. These FT-IR spectra changes indicate that an interaction took place between the protein C=O with the molecules of drugs, and that a partial unfolding of IVIG structure took place in aqueous solution when both of the drugs were added into the protein solution respectively. The differences of FT-IR spectra between IVIG–kaempferol and IVIG–quercetin systems can also be largely due to the effect of 3′-OH substituent of quercetin in comparison with kaempferol. 3′-OH substituent of quercetin may form hydrogen band with amino acid residues of IVIG and subsequently cause a distinct change for the conformation of IVIG.

CD Spectra To obtain a further insight into the changes of secondary structure of IVIG, far-ultraviolet CD spectra were studied for the protein–drug systems. In the far ultraviolet region, such spectra relate to the polypeptide backbone structures. The comparison of the CD spectra for IVIG–kaempferol and IVIG–quercetin with free IVIG in Tris–HCl–NaCl (50 mM, pH 7.40) systems is shown in Fig. 6. The CD spectra of IVIG show a negative position at 216 nm which is relative to its typical β-sheet secondary structure coupled with the contribution of random coil. The negative position at 204 nm, which exists a slight blue shift in aqueous solution, is relative to its type I β-turn secondary structure, while the positive position at 198 nm is relative to its type II β-turn secondary structure coupled with the contribution of α-helix secondary structure. The negative position at 193 nm is relative to random coil coupled with the contribution of β-sheet secondary structure.[34] When kaempferol and quercetin were added into the protein system respectively, the band intensity of typical negative position at 216 nm reduced accompanied by a slight blue shift to 215 nm, suggesting that the component of β-sheet secondary structure decreased accompanied by a transition into random coil. Additionally, the reduction of band intensity at 215 nm for IVIG–quercetin system is smaller than that for IVIG–kaempferol system, suggesting that the β-sheet secondary structural composition of IVIG in the presence of quercetin is higher than that in the presence of kaempferol, which are in good agreement with the results of above FT-IR study. Furthermore, the position of type I β-turn at 204 nm was not observed and the band intensity of type II β-turn position at 198 nm reduced in the CD spectra of both IVIG–drug systems, indicating that β-turn secondary structural compositions decreased in the presence of both drugs in comparison with free IVIG, which are also in good agreement with the results of FT-IR study. On the other hand, there exist some new positive peaks such as 196 nm, 204 nm and 206 nm, which are relative to the splitting of $\pi\pi^*$ transition of α-helix into parallel-polarized and perpendicular-polarized components, so the contribution of α-helix to the band intensity at 198 nm is important. In addition, the changes of CD spectra of IVIG near 193 nm in the absence and in the presence of drugs also indicate a partial unfolding of the protein structure in aqueous solution. However, the typical β structural conformation of IVIG is retentive in the presence of two drugs, so it is predictable that the interactions of IVIG with the two drugs may be reversible and the immunological functions of IVIG may be still retentive, which should be further studied *in vivo*.

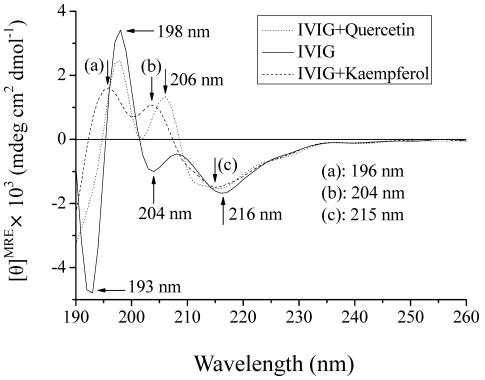

Fig. 6. The Far-UV CD Spectra of IVIG–Kaempferol and IVIG–Quercetin Systems in Aqueous Solution, pH 7.40, 296 K

The number of the amino acid residues of IVIG was taken as 670. The molar concentration of IVIG was 2.0×10^{-5} M, and both the molar concentrations of kaempferol and quercetin were 8.0×10^{-5} M.

The Binding Distance between Drugs and IVIG According to the theory of Förster energy transfer, the efficiency of energy transfer, E, is given by[35]:

$$E=1-F/F_o=R_o^6/(R_o^6+r^6) \quad (5)$$

Where r is the donor–acceptor distance and R_o is the distance at 50% transfer efficiency.[33] F_o and F are the fluorescence intensity of IVIG in the absence and in the presence of drug, respectively.

$$R_o^6=8.8\times10^{-25}K^2n^{-4}\Phi J \quad (6)$$

Where K^2 is the orientation factor related to the geometry of the donor–acceptor of dipole and $K^2=2/3$ for random orientation as in fluid solution[17]; n (=1.336) is the refractive index of medium; Φ is the fluorescence quantum yield of the donor, its value was taken as 0.118[27]; J is the overlap integral of the fluorescence emission spectra of the donor and the absorption spectra of the acceptor. J is given by:

$$J=\frac{\sum F(\lambda)\varepsilon(\lambda)\lambda^4\Delta\lambda}{\sum F(\lambda)\Delta\lambda} \quad (7)$$

Where $F(\lambda)$ is the fluorescence intensity of fluorescence reagent when the wavelength is λ; $\varepsilon(\lambda)$ is the molar absorbance coefficient at the wavelength of λ. From these relationships, J, E and R_o can be calculated, so the value of r can also be calculated.

Figure 7 is the overlaps of the fluorescence spectra of IVIG and the absorption spectra of both drugs when both the molar ratios of drugs to IVIG are 2 to 1 at 296 K. For kaempferol, the value of J calculated according to the above relationships is 2.085×10^{-14} cm^6 $(mol/l)^{-1}$, so the value of R_o is 2.77 nm, and the value of r is 4.30 nm where the value

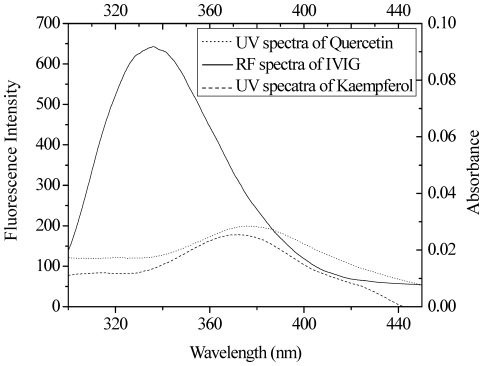

Fig. 7. The Overlaps of the Fluorescence Spectra of IVIG with the Absorption Spectra of Kaempferol and Quercetin at 296 K, pH 7.40

λ_{ex}=283 nm, λ_{em}=337 nm. The molar concentration of IVIG was 1.0 μM, and both the molar concentrations of kaempferol and quercetin were 2.0 μM.

of E is 0.06679. For quercetin, the value of J calculated according to the above relationships is 3.092×10^{-14} cm^6 (mol/l)$^{-1}$, so the value of R_o is 2.96 nm, and the value of r is 4.35 nm where the value of E is 0.09043. The values of r (<7—10 nm) indicate that both the bindings of IVIG to drugs are through exchange energy transfer which will quench the fluorescence of chromophores (mainly the tryptophan residues) in IVIG.[37,38] The value of r between kaempferol with the chromophores of IVIG is shorter than that of quercetin with the chromophores of IVIG, which indicates that kaempferol is more accessible to the hydrophobic clefts of IVIG mainly through hydrophobic forces than quercetin, while quercetin has 3′-OH substituent which may form extra hydrogen band with amino acid residues in comparison with kaempferol, and that there is no exact coherence between the donor–acceptor distance (r) and the affinity constant (K_o). In addition, the efficiency of energy transfer (E) between IVIG with quercetin is higer than IVIG with kaempferol, so it is inferred that it is coherent between the efficiency of energy transfer (E) and the affinity constant (K_o) in the binding of the protein with drugs. IgG comprises of 12 domains, each light chain has two domains (V_L and C_L) and each heavy chain has four domains (V_H, C_H1, C_H2 and C_H3). All the domains of IgG have two cysteine (Cys) residues which form the intradomain disulfide bond and at least one tryptophan (Trp) residue which can protect against the hydrolysis by proteinase.[13,14] Studies of X-ray analysis of crystal structure on the light-chain dimer Mcgλ have proved that V_L has a constant Trp-37 residue and C_L has a constant Trp-152 residue, and both of Trp residues are adjacent to disulfide bonds. Studies of X-ray analysis of crystal structure on the interaction of IgG1Fab′ (New) with VitK_1OH have proved that the end of VitK_1OH is adjacent to the Trp-54 of CDRs of IgG1Fab′ (New).[19] The 3D structure of human IgG in complex with 5-(*para*-nitrophenyl phosphonate)-pentanoic acid downloaded from the Brookhaven Protein Data Bank (PDB entry code 1AJ7) in Fig. 8 shows that Trp-103, Trp-47 and Trp-36 are highly adjacent to the molecules of drugs in these interactions. In the present experiment, the molecules of drugs probably bind to and exchange energy with Trp-103, Trp-47 and Trp-36 residues of IgG, which will quench the fluorescence of the protein. So, the distance (r) calculated here may be the average values between the bound drugs and the tryptophan residues of IgG.

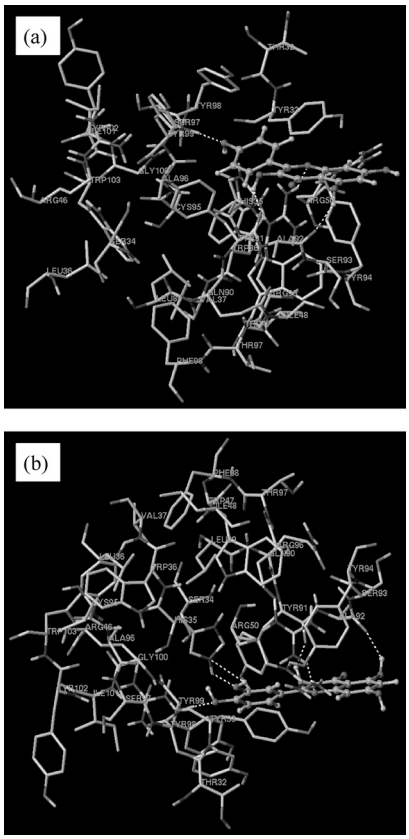

Fig. 8. The Interaction Modes between Human IgG with Kaempferol (a) and Quercetin (b)

The molecule of drug is located in CDR of Fab of IgG. Only residues around 6.5 Å of the drug are displayed. The residues of IgG are represented using capped stick and the drug structure is represented using ball and stick model. The hydrogen bonds are indicated by yellow dash. (Note that these figures are not colored).

Molecular Modeling Study of the Interactions between Human IgG and Drugs IgG has two heavy chains consisting of about 450 amino acid residues and two light chains consisting of about 210—230 amino acid residues. Studies of X-ray analysis of crystal structure on IgG1 (New) have proved that the antigen-binding site distributes over a "shallow cavity" (cleft) with the size of 1.5 nm×0.6 nm×0.6 nm, which is made up of about 10—12 amino acid residues of CDR of Fab, semi-antigen and drugs can be accessible to the cleft and associate with the amino acid residues of CDR with the mode of complementary structure through hydrogen bond, Van der Waals force, electrostatic interaction and hydrophobic interaction, *etc.*[19] There are such two structurally similar "shallow cavities" (clefts) in IgG, *i.e.*, two binding sites for antigens/semi-antigens, which appear higher affinity and specificity and many drugs can bind to, though there are two other binding sites for complements in IgG which appear lower affinity and drugs can also bind to, as indicated by the binding parameters studied in this paper. Here, partial binding parameters of the human IgG–kaempferol and human IgG–quercetin systems were calculated using SGI Fuel workstation. The FlexX program of Sybyl 6.9.1 was used to calculate the interaction modes between drugs and IgG. During docking process, a maximum of 30 conformers were considered for the compounds. The conformers with the lowest binding free energy (for kaempferol–IgG, $\Delta G=-68.97$ kJ mol^{-1}; for quercetin–IgG, $\Delta G=-69.39$ kJ mol^{-1}) were

used for further analysis. Figure 8 shows the interaction modes between the amino acid residues of human IgG with kaempferol and quercetin. As shown in Fig. 8a, there are hydrogen bonds between kaempferol with Tyr-91, Ala-92, Arg-96 and Tyr-99 of IgG, in addition, there are hydrophobic forces between kaempferol with Tyr-33, Tyr-91, Tyr-94, Arg-96, and Tyr-98 of IgG. Figure 8b shows that there are hydrogen bonds between quercetin with His-35, Tyr-91, Ala-92, Arg-96 and Tyr-99 of IgG, in addition, there are hydrophobic forces between quercetin with Tyr-33, Tyr-91, Tyr-94, Arg-96, and Tyr-98 of IgG. It is obvious that there is an extra hydrogen bond between His-35 with 3′-OH substituent of quercetin in comparison with kaempferol, which may be the main reason for their differences of fluorescence spectra, FT-IR spectra and CD spectra between the interactions of kaempferol and quercetin with the protein. However, other effects such as steric coherence and electrostatic interaction at pH 7.40 are not excluded.

Comparison of the Binding Properties of IVIG and HSA to Drugs There are different binding modes and different binding parameters including the binding constants and the binding site numbers between the interactions of IVIG and HSA with drugs due to their different structures and different conformations. A fluorescence spectroscopic study of the interactions of kaempferol with HSA and bovine serum albumin (BSA) by Stern–Volmer method revealed that the binding constants were $1.79\times10^5\,\mathrm{M}^{-1}$ and $8.67\times10^4\,\mathrm{M}^{-1}$, and the Gibbs free energy changes ΔG° were $-27.983\,\mathrm{kJ\,mol}^{-1}$ and $-29.8\,\mathrm{kJ\,mol}^{-1}$, respectively, at 296 K.[17,18] A fluorescence spectroscopic study of the interaction of quercetin with HSA revealed that quercetin molecules bind at a motionally restricted site near tryptophan-214 in the intradomain cleft region of HSA, and the binding constant ($K=1.9\times10^5\,\mathrm{M}^{-1}$) and the Gibbs free energy change ($\Delta G^\circ=-30.12\,\mathrm{kJ/mol}$) for quercetin–HSA interaction have been calculated from the relevant anisotropy data.[15] In the present experiments, the binding constants of IVIG with kaempferol and quercetin calculated are $1.032\times10^4\,\mathrm{M}^{-1}$ and $1.849\times10^4\,\mathrm{M}^{-1}$ ($n=2$) at 296 K, respectively. These indicate that the bindings of HSA to kaempferol and quercetin are stronger than that of IVIG to them, and there will be a competitive reaction between HSA and IVIG binding to kaempferol and quercetin in blood.

Conclusion

The interactions of kaempferol and quercetin with IVIG have been studied by fluorescence quenching, FT-IR spectra and CD spectra. From above experiments we can obtain that IVIG binds to kaempferol and quercetin with an average affinity constants at $1.032\times10^4\,\mathrm{M}^{-1}$ and 1.849×10^4 ($n=$ 2296 K), respectively. The binding of IVIG with quercetin is stronger than that of IVIG with kaempferol. The molecules of kaempferol and quercetin are mainly located in CDRs of Fab of IgG. The bindings of IVIG to both of drugs are of non-specific and weak interactions with respect to the other strong ligand–protein complexes with binding constants ranging from 10^6 to $10^8\,\mathrm{M}^{-1}$. The effect of 3′-OH substituent in quercetin is distinct between the interactions of IVIG with kaempferol and quercetin for the secondary structure of the protein. The observed spectral changes indicate a partial unfolding of the protein structure, but the typical β structural conformation of IVIG is retentive and the immunological function of IVIG may be also retentive in the presence of both drugs in aqueous solution, which should be further studied *in vivo*. The average binding distances between the chromophores of IVIG with kaempferol (4.30 nm) and quercetin (4.35 nm) are obtained. IVIG can serve as transport protein (carrier) for kaempferol and quercetin, but the bindings of HSA to them are stronger than that of IVIG to them, and there are competitive reactions between HSA and IVIG binding to them in blood.

Acknowledgements This work was supported by the National Natural Science Foundation of China (20475023), Gansu NST (3ZS 041-A25-016), and the Gansu Province College and University Science and Research Project for Supervisor of Graduate Students (0510-06).

References

1) Bayry J., Lacroix-Desmazes S., Kazatchkine M. D., Kaveri S. V., *Nat. Clin. Pract. Rheum.*, **3**, 262—272 (2007).
2) Bayry J., Misra N., Latry V., Prost F., Delignat S., Lacroix-Desmazes S., Kazatchkine M. D., Kaveri S. V., *Transfusion Clinique et Biologique*, **10**, 165—169 (2003).
3) Shoenfeld Y., Fishman P., *Int. Immunol.*, **11**, 247—252 (1999).
4) Shoenfeld Y., Levy Y., Fishman P., *Isr. Med. Ass. J.*, **3**, 698—699 (2001).
5) Phuphanich S., Brock C., *J. Neurooncol.*, **81**, 67—69 (2007).
6) Rowland G. F., Axton C. A., Baldwin R. W., Brown J. P., Corvalan J. R. F., Embleton M. J., Gore V. A., Hellström I., Hellström K. E., Jacobs E., Marsden C. H., Pimm M. V., Simmonds R. G., Smith W., *Cancer Immunol. Immun.*, **19**, 1—7 (1985).
7) Yu Z. Y., Tang Z. Y., Ma J. Y., *Tumor* (Shanghai), **9**, 154—156 (1989).
8) Lutz H. U., Stammler P., Jelezarova E., Nater M., Spath P. J., *Blood*, **88**, 184—193 (1996).
9) Liu Y. C., Yang Z. Y., Du J., Yao X. J., Zheng X. D., Lei R. X., Liu J. N., Hu H. S., Li H., *Int. Immunopharmacol.*, **8**, 390—400 (2008).
10) Lev S., Gilburd B., Lahat N., Shoenfeld Y., *Eur. J. Int. Med.*, **13**, 101—103 (2002).
11) Westemark J., Kahari V. M., *FASEB J.*, **13**, 781—792 (1999).
12) Liu J. Q., Tian J. N., Hu Z. D., Chen X. G., *Biopolymers*, **73**, 443—450 (2004).
13) Liu Y. C., He W. Y., Gao W. H., Hu Z. D., Chen X. G., *Int. J. Biol. Macromol.*, **37**, 1—11 (2005).
14) Liu Y. C., Lei R. X., Hu Z. D., Chen X. G., Shen F. L., Jing J., *Spectroscopy Lett.*, **39**, 265—284 (2006).
15) Sengupta B., Sengupta P. K., *Biochem. Biophys. Res. Commun.*, **299**, 400—403 (2002).
16) Sengupta B., Sengupta P. K., *Biopolymers (Biospectroscopy)*, **72**, 427—434 (2003).
17) Tian J. N., Liu J. Q., Tian X., Hu Z. D., Chen X. G., *J. Mol. Stuct.*, **691**, 197—202 (2004).
18) Tian J. N., "Study on Interaction of Four Active Components in Chinese Traditional Medicines with Proteins," Doctoral Dissertation of Lanzhou University, Lanzhou, 2004.
19) Jiang S. Y., Zhang L. Y., "Immunochemistry," Shanghai Medical University Press, Shanghai, 1996.
20) Bagatolli L. A., Kivatinitz S. C., Fidelio G. D., *J. Pharm. Sci.*, **85**, 1131—1132 (1996).
21) Yang M. M., Yang P., Zhang L. W., *Chinese Sci. Bull.*, **9**, 31—36 (1994).
22) Dong A. C., Huang P., Caughey W. S., *Biochemistry*, **29**, 3303—3306 (1990).
23) Purcell M., Neault J. F., Tajumir-Riahi H. A., *Biochim. Biophys. Acta*, **1478**, 61—68 (2000).
24) Tayyab S., Soghra K. H., Haq S. K., Sabeeha, Aziz M. A., Khan M. M., Muzammil S., Mohammad M. K., Muzammil S., *Int. J. Biol. Macromol.*, **26**, 173—180 (1999).
25) SYBYL Software, Version 6.9.1, St. Louis, Tripos Associates Inc., 2003.
26) Yuan T., Weljie A. M., Vogel H. J., *Biochemistry*, **37**, 3187—3195 (1998).
27) Yang P., Gao F., "Biological and Inorganic Chemistry," Science Press, Beijing, 2002.
28) Hasemann C. A., Capra J. D., *J. Biol. Chem.*, **266**, 7626—7632 (1991).

29) Amit A. G., Mariazza R. A., Phillips S. E., Poljak R. J., *Science*, **233**, 747—753 (1986).
30) Corper A. L., Sohi M. K., Bonagura V. R., Steinitz M., Jefferis R., Feinstein A., Beale D., Sutton B. J., *Nat. Struct. Biol.*, **4**, 374—381 (1997).
31) Ouameur A. A., Marty R., Tajmir-Riahi H. A., *Biopolymers*, **77**, 129—136 (2005).
32) Wi S., Pancoka P., Vogel T. A., *Biospectroscopy*, **4**, 93—99 (1998).
33) Rahmelow K., Hubner W., *Anal. Biochem.*, **241**, 5—11 (1996).
34) Fasman G. D., "Circular Dichroism and the Conformational Analysis of Biomolecules," Plenum Press, New York, 1996, pp. 25—380.
35) Förster T., "Modern Quantum Chemistry," Vol. 3, ed. by Sinanoglu O., Academic Press, New York, 1966, p. 93.
34) Kassi S., Horie T., Mizuma T., Awazu S., *J. Pharm. Sci.*, **76**, 387—392 (1987).
35) Marty A., Boiret M., Deumie M., *J. Chem. Educ.*, **63**, 365—366 (1986).
36) Chen G. Z., Huang X. Z., Zheng Z. Z., Xu J. G., Wang Z. B., "Fluorometry," 2nd ed., Science Press, Beijing, 1990.